

needed to ascertain the robustness of the analytical method, the lack of spectral interference from plasma-type emission is certainly promising.

CONCLUSION

Excimer laser fragmentation fluorescence spectroscopy using a 193 nm ArF excimer laser was used to detect atomic Pb emission from solid PbNO₃ and PbNO₃ mixed into a soil. The detection method differs from other solid ablation processes in that lower laser fluences can be used where there is no plasma generation and subsequent broadband emission; fluences above 2 J/cm² resulted in plasma formation. The detection limit for PbNO₃ in a single soil type is about 200 ppm, achieved with minimal sample preparation and an analysis time on the order of a minute. The technique holds promise as a rapid and sensitive method for processing soil samples for assessing exposures or the effectiveness of soil remediation.

ACKNOWLEDGMENT

This work was supported by the Environmental Health Sciences Superfund Basic Research Program (Grant Number P42ESO47050-01) from the National Institute of Environmental Health Sciences, NIH, with funding provided by the EPA. The authors thank the Wood-Calvert Chair in Engineering for additional support. The contents of the work are solely the responsibility of the authors and do not necessarily represent the official views of NIEHS, NIH, or EPA.

1. USEPA, 747-R-97-006 (1998).
2. H. L. Needleman, C. Gunnoe, A. Leviton, R. Reed, H. Peresie, C. Maher, and P. Barrett, *N. Engl. J. Med.* **300**, 689 (1979).
3. G. A. Wasserman, X. Liu, N. J. Lolocono, P. Factor-Litvak, J. K. Kline, D. Popovac, N. Morina, A. Musabergovoc, N. Vrenezi, S. Capuni-Paracka, V. Lekic, E. Preteni-Redjepi, S. Hadzialjevic, V. Salkovich, and J. H. Graziano, *Environ. Health Perspect.* **105**, 956 (1997).
4. F. Hilbk-Kortenbruck, N. Reinhard, P. Wintjens, F. Heinz, and C. Becker, *Spectrochim. Acta, Part B* **56**, 933 (2001).
5. F. Capitelli, F. Colao, M. R. Provenzano, R. Fantoni, G. Brunetti, and N. Senesi, *Geoderma* **106**, 45 (2002).
6. V. Bulatov, R. Krasniker, and I. Schechter, *Anal. Chem.* **70**, 5302 (1998).
7. C. J. Damm, D. Lucas, R. F. Sawyer, and C. P. Koshland, *Chemosphere* **42**, 655 (2001).
8. S. G. Buckley, D. Lucas, C. P. Koshland, and R. F. Sawyer, *Combust. Sci. Technol.* **118**, 169 (1996).
9. C. S. McEnally, D. Lucas, C. P. Koshland, and R. F. Sawyer, *Appl. Opt.* **33**, 3977 (1994).
10. B. L. Chadwick, G. Domazetis, and R. J. S. Morrison, *Anal. Chem.* **67**, 710 (1995).
11. R. C. Sausa, A. J. Alfano, and A. W. Miziolek, *Appl. Opt.* **26**, 3588 (1987).
12. N. J. O'Donovan, M.S. Thesis, Mechanical Engineering Department, University of California at Berkeley, Berkeley, California (2002).
13. S. G. Buckley, C. J. Damm, W. M. Vitovec, L. A. Sgro, R. F. Sawyer, C. P. Koshland, and D. Lucas, *Appl. Opt.* **37**, 8382 (1998).
14. W. F. Ho, C. W. Ng, and N. H. Cheung, *Appl. Spectrosc.* **51**, 87 (1997).
15. D. S. Tomson and D. M. Murphy, *Appl. Opt.* **32**, 6818 (1993).
16. J. E. Carranza and D. W. Hahn, *Anal. Chem.* **74**, 5450 (2002).
17. A. Eppler, D. A. Cremers, D. D. Hickmott, M. J. Ferris, and A. C. Koskelo, *Appl. Spectrosc.* **60**, 1175 (1996).
18. R. Wisbrun, I. Schechter, R. Niessner, H. Schroder, and K. L. Kompa, *Anal. Chem.* **66**, 2964 (1994).
19. USEPA, 40 CFR Part 745 (2001).

An Internal Standardization Procedure for Spectrally Resolved Fluorescence Lifetime Imaging

QUENTIN S. HANLEY* and V. RAMKUMAR†

Department of Biological and Chemical Sciences, University of the West Indies, Cave Hill Campus, St. Michael, Barbados

Index Headings: **Fluorescence lifetime imaging; FLIM; Spectrally resolved FLIM; Frequency domain; Standardization; Fluorescence.**

INTRODUCTION

Fluorescence lifetime imaging (FLIM) is typically done in a two-dimensional imaging mode without measuring the entire lifetime spectrum. The introduction of an imaging spectrograph into the detection path of the lifetime instrument allows the lifetime spectrum to be observed, including the lifetime signature of any excitation light passing through the emission filter of the microscope. Excitation light leaking into the detection path of a conventional FLIM system is detrimental to the measurement of the lifetimes, since it causes a variable mixing of a short lifetime component into the data. However, by intentionally allowing excitation laser light to enter a spectrally resolved FLIM (sFLIM) detection system, an internal standardization may be provided by comparing the modulation depth and phase shift of the laser light to that of a standard. Such an approach stabilizes the lifetime measurement obtained from a system over time and can reduce the time between measurements by eliminating external standardization. Long-term stabilization is particularly important in drug screening instruments requiring a combination of high-speed and high-stability measurements. Internal standardization can be implemented in sFLIM using a scattering surface and a holographic notch filter. Although this light does not travel the same optical path through the microscope as the fluorescence excitation and emission light, the path length difference can be calibrated, and following calibration it may be used to increase the speed and stability of spectrally resolved FLIM measurements. When compared directly to an external standardization procedure improved accuracy and precision were observed while potentially improving the throughput of sFLIM instrumentation.

Fluorescence lifetime imaging in either the time¹⁻³ or frequency⁴⁻⁶ domain is becoming a mature method for investigating proximity relationships in intact cellular systems.^{7,8} A variety of commercial instruments are available as additions to wide field and confocal microscopes and approaches have been described for the analysis of mixtures⁹ and functional imaging.^{7,10,11} In the time do-

Received 3 August 2004; accepted 11 October 2004.

* Author to whom correspondence should be sent. E-mail: qhanley@uwichill.edu.bb.

† Current address: Department of Chemistry, Indian Institute of Technology Madras, Chennai, India.

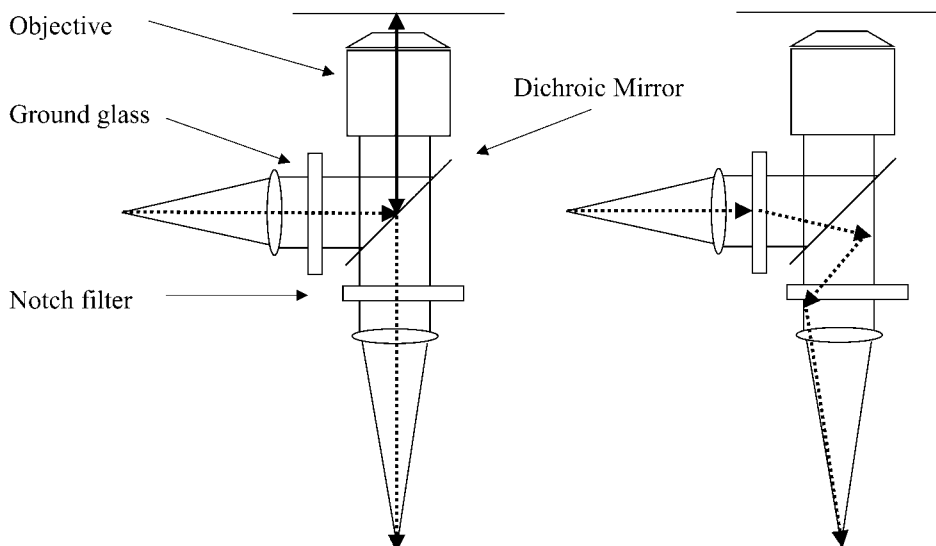


FIG. 1. Illustration of the optical paths for (a) excitation and emission of fluorescence and (b) scattered light. The solid line in the excitation and emission diagram (a) indicates both directions of the optical path that are not shared by the scattered light. In the Nikon TE-300, the distance from the midpoint of the dichroic mirror and the object plane of the microscope is approximately 13 cm. The scattered light path illustrated (b) is one of many possible paths and is shown for illustration only.

main, the response of a region of a preparation to a pulse of light is observed. In the frequency domain, the modulation and phase shift of fluorescence light observed from a preparation is compared to the response from a standard. For either approach, the light collected passes through an emission filter removing excitation light and regions of the emission spectrum that are not of interest. More recently, frequency domain spectrally resolved fluorescence lifetime imaging (sFLIM) has been described.¹² Among the many advantages of the method is the ability to observe the full emission spectrum of the system being studied, which might include many fluorophores.

Lifetime imaging could be of interest in the field of drug discovery to assess donor–acceptor relationships on a large scale provided that it can be shown to be fast and reliable. Moving spectrally resolved fluorescence lifetime imaging to the level of a routine automated measurement would allow single or multiple donor–acceptor pairs to be followed simultaneously. However, little is known about the long-term stability, accuracy, and precision of either FLIM or sFLIM. No benchmarks are available for sample throughput and no inter-laboratory comparisons have been done on standard samples. Considerable theoretical work on approaches to obtaining optimal signal-to-noise ratios (S/N) in FLIM has been reported previously.¹³ However, other factors influencing the stability of frequency domain lifetime imaging measurements have not been investigated extensively and much of what is known remains anecdotal. Experience has shown that in some systems temperature-related phase drift in acousto-optic modulators can be a problem. Frequent calibration can reduce instrumental drift;¹⁴ however, this increases the analysis time. While some of the problems associated with phase drift may improve with the introduction of new modulation technologies such as modulated LED light sources and other types of modulators, these tech-

nologies have not been fully evaluated for long-term stability and applications remain where a laser is desirable.

This note is concerned with investigating the stability of spectrally resolved frequency domain lifetime measurements using laser excitation sources and increasing the throughput of the method. A direct comparison between external and internal standardization procedures is made. This is done by observing the phase and modulation depth of laser light intentionally introduced into the detection path of the sFLIM and comparing the result to that obtained by conventional calibration methods.

Distance-Dependent Phase Shift. A typical fluorescence microscope incorporates a filter set consisting of an excitation filter, a dichroic mirror, and an emission filter. This arrangement provides excitation light to stimulate fluorescence; the excitation light is later removed from the detection path by the emission filter. In the implementation of the spectroscopic FLIM system, the excitation filter is removed and the emission filter is replaced with a holographic notch filter. These filters are designed for light arriving perpendicular to the surface. As the angle of the incident beam deviates from perpendicular, such as will happen from light scattered by the ground glass disk, it can pass the notch filter. This light carries information about the phase shift of the incident light.

The point to note, however, is that this light does not travel the same path as the light used to excite the sample (Fig. 1). The majority of the laser light passing the notch filter is scattered directly into the detection path without traveling to and from the object plane of the microscope. This results in a path length difference between the light exciting fluorescence in the microscope and the internal reference. These differences can be accounted for by noting that sinusoidally modulated light travels a fixed distance, d , through a medium during a single period of modulation. The distance traveled is related to the refractive index, n , the frequency of modulation, f , and the speed of light, c . In air, the relationship simplifies to:

$$d = \frac{c}{f} \quad (1)$$

Equation 1 indicates that for a light source modulated at 80 MHz, the distance traveled is about 3.75 meters per period. Thus, the difference between the position of zero phase calculated with the use of a standard and that measured from laser light leaking through a notch filter will be: (1) insensitive to small adjustments in focus as this is small relative to the distance per period, (2) easily calibrated, and (3) once calibrated, no further calibration should be needed. As such, it can serve as an internal reference for subsequent measurements.

The modulation and phase lifetimes for single component decays can be computed from the modulation depth and the phase shift.

$$\tau_m = \omega^{-1} \sqrt{\frac{1}{m^2} - 1} \quad (2)$$

$$\tau_\phi = \omega^{-1} \tan \phi \quad (3)$$

In practical implementations of the frequency domain technique, measured modulation depths and phase shifts must be adjusted to account for the modulation and phase position of the excitation light. This is normally done by measuring a lifetime standard such as Rhodamine 6G or by measuring the modulation depth and phase shift of the excitation light directly using a reflective surface or scattering medium in the object plane of the instrument. In the case of a lifetime standard, the modulation and phase shift of a mono-exponential external standard system can be computed by rearranging Eqs. 2 and 3:

$$m_{\text{std,calc}} = \frac{1}{\sqrt{1 + \omega^2 \tau^2}} \quad (4)$$

$$\phi_{\text{std,calc}} = \tan^{-1}(\omega\tau) \quad (5)$$

where $m_{\text{std,calc}}$ is the calculated modulation depth, $\phi_{\text{std,calc}}$ is the calculated phase shift, τ is the fluorescence lifetime of the standard, and ω is $2\pi f$, where f is the frequency of modulation in Hz. Calibrated corrections to the modulation depth and phase shift can then be computed from data measured as a calibration data set:

$$m_{\text{corr}} = \frac{m_{\text{std,calc}}}{m_{\text{std,meas}}} m_{\text{laser,meas}} \quad (6)$$

$$\phi_{\text{corr}} = \phi_{\text{laser,meas}} - \phi_{\text{std,meas}} + \phi_{\text{std,calc}} \quad (7)$$

where $m_{\text{std,meas}}$ is the measured modulation depth for the calibration sample, $m_{\text{laser,meas}}$ is the measured modulation depth of the laser light, $\phi_{\text{std,meas}}$ is the measured phase of the standard, and $\phi_{\text{laser,meas}}$ is the measured phase of the laser light. Correction for the experimental modulation and phase can then be applied to subsequent measurements.

$$m_{\text{samp,corr}} = \frac{m_{\text{samp,meas}}}{m_{\text{laser,int}}} m_{\text{corr}} \quad (8)$$

$$\phi_{\text{samp,corr}} = \phi_{\text{samp,meas}} - \phi_{\text{laser,int}} + \phi_{\text{corr}} \quad (9)$$

where $m_{\text{samp,meas}}$ is the measured modulation depth for the sample, $m_{\text{laser,int}}$ is the modulation depth of the laser internal standard, $\phi_{\text{samp,meas}}$ is the measured phase of the

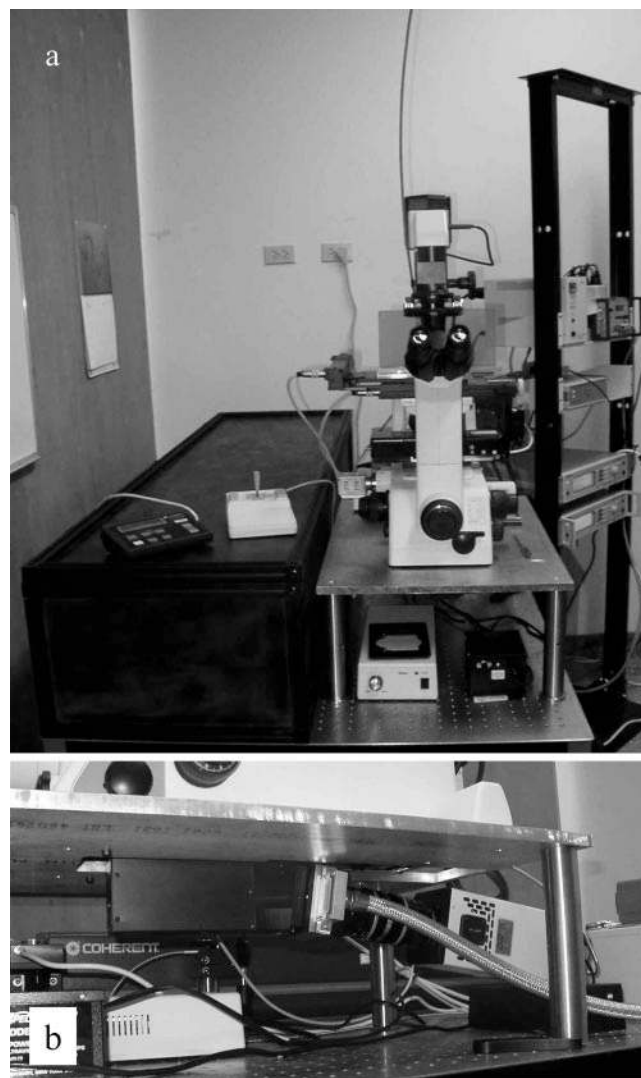


FIG. 2. (a) Image of the system. Black enclosure on the left side of image contains the Ar ion laser, AOM, laser shutter, and mode scrambler. The laser light is relayed to the back of the microscope by an optical fiber. The microscope assembly includes the programmable x-y stage and the camera, spectrograph, and intensifier assembly. Signal generators are located to the right to the back of the microscope. (b) The CCD camera, intensifier, relay optics, and spectrograph are mounted underneath the microscope.

sample, and $\phi_{\text{laser,int}}$ is the phase of the laser internal standard. The reference given by the laser within every spectral lifetime image provides the internal calibration.

EXPERIMENTAL

The spectrally resolved lifetime imaging system was built as an accessory to an inverted fluorescence microscope (E-300 Quantum; Nikon, New York, NY) (Figs. 1 and 2). Images were collected using a charge-coupled device (CCD) camera (SensiCam Long Exposure; PCO Computer Optics GmbH, Kelheim, Germany) attached to a modulatable image intensifier (High Rate Imager; Kentech Instruments Limited, United Kingdom). Images were relayed from the image intensifier to the CCD camera using a pair of camera lenses (Nikon 50 mm f/1.8; B & H Photo, New York, NY). The intensifier was attached to the microscope via an imaging spectrograph (PARISS;

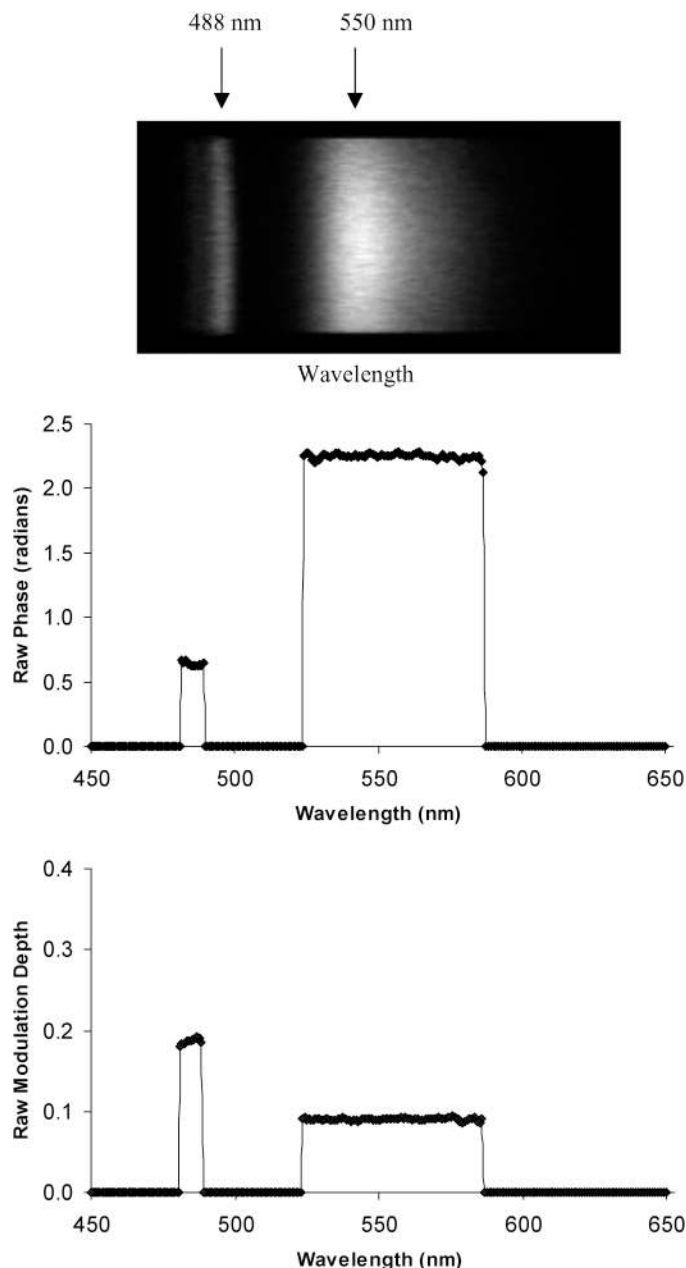


FIG. 3. Raw data image from sFLIM acquisition. The image shows a narrow band from the scattered laser light and a broad band of fluorescence from the rhodamine 6G. The graphs show the raw average phase and modulation depth for a single lifetime data set. They show the distinct signature of the rhodamine 6G and scattered laser light. Peak values at the beginning and end of the rhodamine region of the phase data are an artifact of the threshold algorithm used to process the data.

Lightform Inc., Hillsborough, NJ), which provided the spectroscopic resolution. Illumination was provided by an Ar⁺ ion laser (I90C-6; Coherent, Santa Clara, CA) tuned to 488 nm. Light from the laser passed through an acousto-optic modulator (AOM) (SSM-402F8-1; IntraAction Corp, Belwood, IL). The AOM was driven with a phase-locked signal generator set to a frequency of 40.15 MHz (2023A; IFR, Wichita, KS) leading to optical modulation at 80.30 MHz. The AOM signal generator was frequency and phase locked to a second signal generator, which provided the frequency signal for the modulatable intensifier. The output of the signal generator was amplified using a

broadband RF power amplifier (PA-4; IntraAction Corp, Belwood, IL) and used to drive the AOM. The zero order light from the AOM was selected and relayed through a multimode optical fiber (PCU40-2-SS-GT; Multimode Fiber Optics, East Hanover, NJ) to the microscope illumination port. The optical fiber was mechanically shaken at 50 Hz with the assistance of an acoustic speaker and a 6 V transformer to scramble the modes. An automated multi-well plate sample changer was implemented with an x-y scanning stage (Scan IM 120 × 100; Märzhäuser, Wetzlar, Germany).

Data collection consisted of an image series in which each image was taken in a set of 16 phase steps 22.5° apart. Following each image series in which a sample was measured, a standard was acquired. Acquisition of a measurement consisting of sample and standard data sets typically took ~5–10 s, including the time spent to change sample position.

Calibration Samples. A series of 1 μM solutions of Rhodamine 6G (Rhodamine 590 Chloride, Exciton, Dayton, OH, lot #60060) were introduced into the wells of a plastic-bottomed 384-well plate (Packard ViewPlate-384, Perkin Elmer Corp.). These samples were excited using the 488 nm line of the Ar⁺ ion laser and observed using a 505 nm dichroic mirror and a 488 nm holographic notch filter (HNF-488.0; Kaiser Optical Systems, Ann Arbor, MI).

RESULTS AND DISCUSSION

A rhodamine solution measured in the system exhibited distinct regions consisting of scattered light from the laser and rhodamine 6G (Fig. 3). Analysis of a series of such images indicated an “excess” phase delay of 0.502 ± 0.008 radians in the system due to the extra distance traveled to and from the object plane of the microscope. Using Eq. 1 and a modulation frequency of 80.30 MHz, the extra distance traveled by the excitation light was computed to be ~30 cm. This corresponds to an extra travel time of ~1 ns for the light exciting fluorescence in the microscope. A similar analysis of the modulation depths indicated that at the point of observation the scattered laser light was ~10% demodulated relative to the point where it excited rhodamine 6G.

The samples of the rhodamine solution in the 384-well plate were measured over the course of 1.5 hours. This implies a rate of ~4 samples per minute including the measurement of a standard well. Two approaches to the measurement of the modulation and phase lifetimes were compared: (1) Measurement relative to a single standard taken at the beginning of the measurements (Fig. 4). (2) Measurement of the sample using the laser light as a reference. The internal standard method gave $\tau_m = 4.10 \pm 0.04$ ns and $\tau_\phi = 4.08 \pm 0.09$ ns, while the external standardization method resulted in $\tau_m = 4.06 \pm 0.04$ ns and $\tau_\phi = 4.26 \pm 0.15$ ns. This indicates that the internal standardization method gives similar or better results while increasing the accuracy and throughput of the measurement. While neither method showed evidence of significant drift over the period of measurement, the internally standardized approach showed fewer signs of systematic errors and, in the case of the phase lifetimes, improved precision. Three points are worth noting. (1)

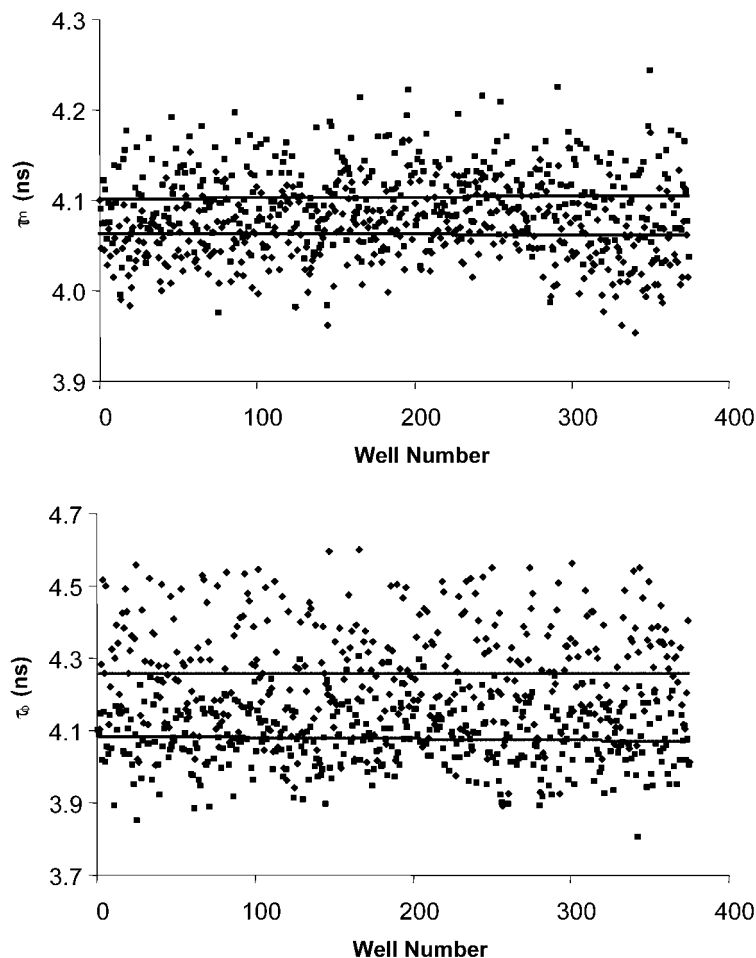


FIG. 4. Comparison of internal and external standardization procedure for a series of uniform solutions in a 384-well plate. The internal standard procedure (■) showed better stability over time than the external procedure (◆).

The external standard consisted of a single standard at the beginning of the plate. This type of measurement gives systematic errors with sensitive dependence on the single measurement of the standard at the beginning of the plate. (2) The increased variation in the phase lifetime indicates that phase “jitter” is substantially reduced using the internal standardization procedure. (3) Use of the internal standardization procedure indicates that the alternating collection of a standard following each sample is not necessary, which would improve the throughput of sFLIM measurement to <8 samples/min in the system described.

CONCLUSION

The present study indicates that a relatively simple and desirable introduction of a holographic notch filter into the optical arrangement of a spectrally resolved FLIM system results in a stabilization of the lifetime measurements over time. The notch filter blocks most of the excitation light and allows the widest spectral range for the emitted fluorescence and, hence, gives the greatest versatility. A few minor drawbacks to the method should also be noted. The primary limitation of the approach is that the fraction of scattered light through the filter is constant for a particular set of components and arrangement. This will result in a limited dynamic range for the

measurements since the intensity of fluorescence collected will vary with individual preparations. Within the dynamic range restrictions imposed by this condition, the method has several advantages:

- 1) The calibration should be stable over time and is valid after turning the system off and back on.
- 2) It removes the requirement of regularly measuring a standard solution over the course of a long series of measurements, which could give stability over weeks of repetitive measurements.
- 3) The standard is collected under the same conditions and coincident in time with the sample.

The optical arrangement described here is a relatively simple modification of systems commonly in use for conventional fluorescent lifetime imaging. It consists of installing a spectrograph and a notch filter and gives considerable additional information about the sample under study. The arrangement could also be used to good effect in cuvette systems to obtain convenient access to spectrally resolved lifetime measurements.

1. J. P. Knemeyer, D. P. Herten, and M. Sauer, *Anal. Chem.* **75**, 2147 (2003).
2. J. Sytsma, J. M. Vroom, C. J. De Grauw, and H. C. Gerritsen, *J. Microsc.* **191**, 39 (1998).

3. A. V. Agronskaia, L. Tertoolen, and H. C. Gerritsen, *J. Phys. D* **36**, 1655 (2003).
4. T. W. J. Gadella, Jr., R. M. Clegg, and T. M. Jovin, *Bioimaging* **2**, 139 (1994).
5. E. B. V. Munster and T. W. J. Gadella, Jr., *J. Microsc.* **213**, 29 (2004).
6. M. J. Booth and T. Wilson, *J. Microsc.* **214**, 36 (2004).
7. P. J. Verveer and P. I. H. Bastiaens, *J. Microsc.* **209**, 1 (2003).
8. P. J. Verveer, F. S. Wouters, A. R. Reynolds, and P. I. H. Bastiaens, *Science (Washington, D.C.)* **290**, 1567 (2000).
9. A. H. A. Clayton, Q. S. Hanley, and P. J. Verveer, *J. Microsc.* **213**, 1 (2004).
10. P. J. Verveer, A. Squire, and P. I. H. Bastiaens, *J. Microsc.* **202**, 451 (2000).
11. P. J. Verveer, A. Squire, and P. I. H. Bastiaens, *J. Microsc.* **202**, 451 (2001).
12. Q. S. Hanley, D. J. Arndt-Jovin, and T. M. Jovin, *Appl. Spectrosc.* **56**, 155 (2002).
13. J. Philip and K. Carlsson, *J. Opt. Soc. Am.* **20**, 368 (2003).
14. Q. S. Hanley, V. Subramaniam, D. J. Arndt-Jovin, and T. M. Jovin, *Cytometry* **43**, 248 (2001).